RSC
Medicinal Chemistry

ROYAL SOCIETY
OF **CHEMISTRY**
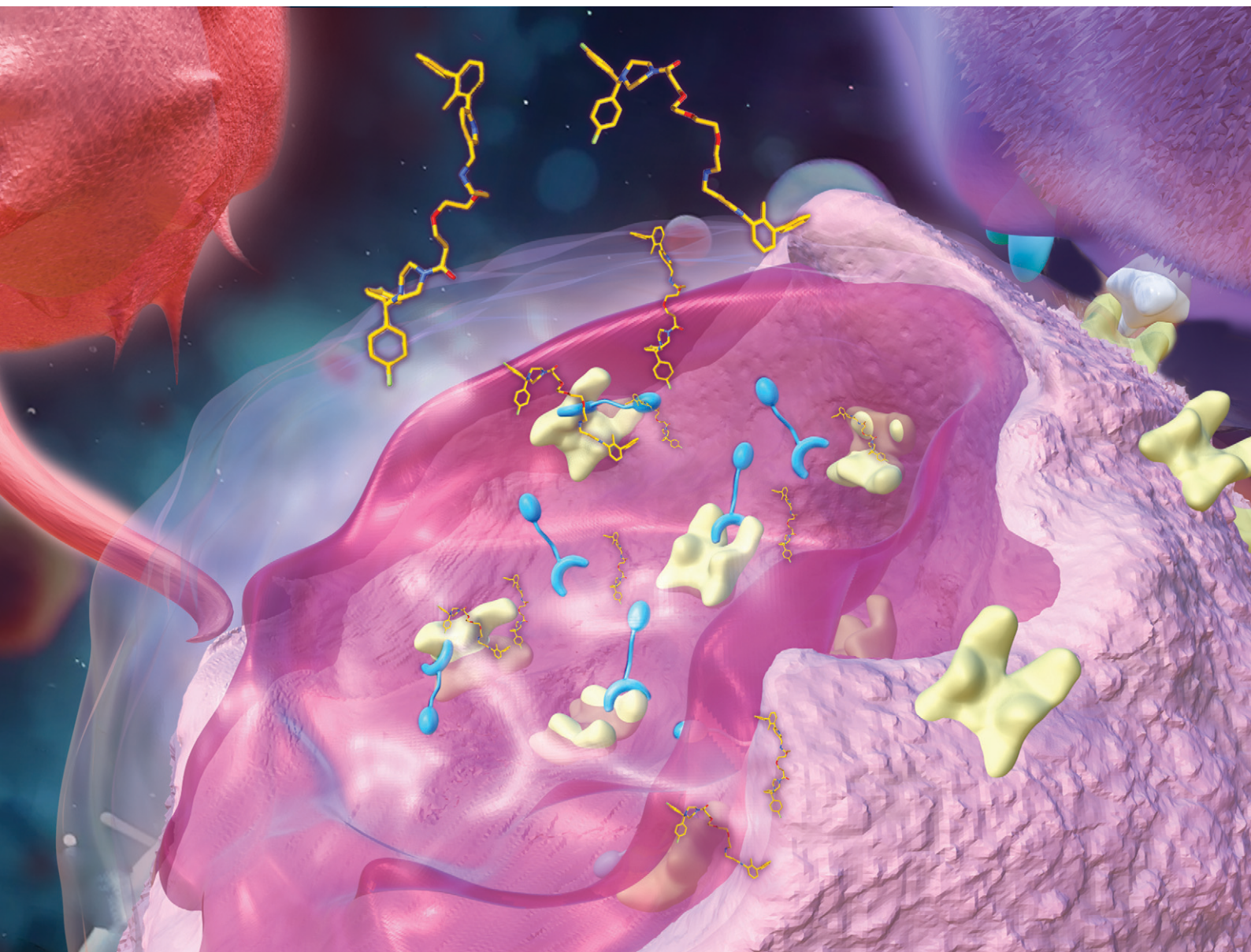
RESEARCH ARTICLE
Jinming Zhou *et al.*
A novel hydrophobic tag leads to the efficient degradation
of programmed death-ligand 1

Check for updates

A novel hydrophobic tag leads to the efficient degradation of programmed death-ligand 1†

Jieke Gao,‡[a] Yongli Xie,‡[b] Jiantao Zhang,‡[a] Huirong Chen,[a] Yan Zou,[a] Shan Cen[b] and Jinming Zhou ID *[a]

The interaction of PD-L1 and PD-1 transmits the inhibitory signal to reduce the proliferation of antigen-specific T-cells in lymph nodes. The expression of PD-L1 confers a potential escaping mechanism of tumors from the host immune system. Blocking the interaction of PD-1 and PD-L1 enables tumor-reactive T cells to overcome regulatory mechanisms and induce an effective antitumor response. The hydrophobic tag tethering degrader (HyTTD) contains a hydrophobic moiety, binding to the protein of interest (POI) to mimic the misfolding state of the POI, thereby inducing the degradation of POI. In this work, using the HyTTD strategy, we selected the diphenylmethyl derivatives as the PD-L1 binding motif for PD-L1 to develop the degraders for PD-L1, and multiple hydrophobic tags were attached. As a result, two HyTTDs **Z2d** and **Z3d** efficiently decreased the protein level of PD-L1 in both NCI-H460 and HT-1080 cells with low cytotoxicity. Meanwhile, the reduction of PD-L1 protein levels by **Z2d/Z3d** was counteracted by **MG132**, which indicated that **Z2d/Z3d** degraded PD-L1 through the proteasome pathway. Moreover, the molecular modeling results indicated that the HyT group of **Z2d** or **Z3d** extended the surface of the protein to mimic the misfold. Importantly, our work also identified a novel HyT, which could be applied to develop the HyTTD for other target proteins.

Introduction

Overexpression of programmed cell death protein 1 (PD-1) leads to the inactivation of T cell effectors and causes the immune escape of cancer cells.[1,2] Programmed death-ligand 1 (PD-L1) is the principal ligand of PD-1 (Fig. 1A), which binds to PD-L1 and transmits the inhibitory signal to reduce the proliferation of antigen-specific T-cells in lymph nodes.[3,4] Therefore, the expression of PD-L1 confers a potential escaping mechanism from the host immune system.[5,6] Blocking the interaction of PD-1 and PD-L1 removes the inhibitory signals of T-cell activation, which enables tumor-reactive T cells to induce an effective antitumor response.[4,6] The anti-PD-L1 antibodies like avelumab, atezolizumab, or durvalumab exhibit significant clinical efficacy by blocking the binding of PD-L1 with PD-1.[7,8] However, antibody-based drugs have multiple drawbacks, including low oral bioavailability, high price, and inducing immune-related adverse effects, thereby limiting the clinical application of PD-L1/PD-1 monoclonal antibodies. Therefore, the development of small-molecular PD-1/PD-L1 inhibitors has attracted huge attention in oncoimmunotherapy.[9,10]

Various small-molecular PD-1/PD-L1 blockers have been reported, especially the compounds with the biphenyl core structure, which bind to PD-L1 and induce the formation of the PD-L1 dimer to block the interaction between PD-1 and PD-L1.[10–15] Targeted protein degradation (TPD) is an efficient strategy to develop degraders, which not only inhibit the protein's function *via* the traditional occupying mode but disable the target through catalytically degrading the target.[16–19] Previously, based on the PROTACs technology, two types of PD-L1 degraders linked with the cereblon ligand were developed and indicated moderate degradation potency (Fig. 1).[20,21] Hydrophobic tag tethering degrader (HyTTD) contains a moiety specifically binding with the protein of interest (POI), a hydrophobic moiety (such as HyT13, HyT16, HyT21, or HyT22, shown in Fig. 1C), and a linker between two moieties, which binds to POI to mimic the protein misfolding, thereby inducing the degradation of POI (Fig. 1).[17,22–24] Herein, using the HyTTD strategy, we developed the degraders for PD-L1 protein. Importantly, a novel hydrophobic tag (HyT) was developed, which led to the efficient degradation of PD-L1.

[a] *Key Laboratory of the Ministry of Education for Advanced Catalysis Materials, Department of Chemistry, Zhejiang Normal University, 688 Yingbin Road, Jinhua 321004, P. R. China. E-mail: zhoujinming@zjnu.edu.cn*
[b] *Institute of Medicinal Biotechnology, Chinese Academy of Medical Science, Beijing, China*
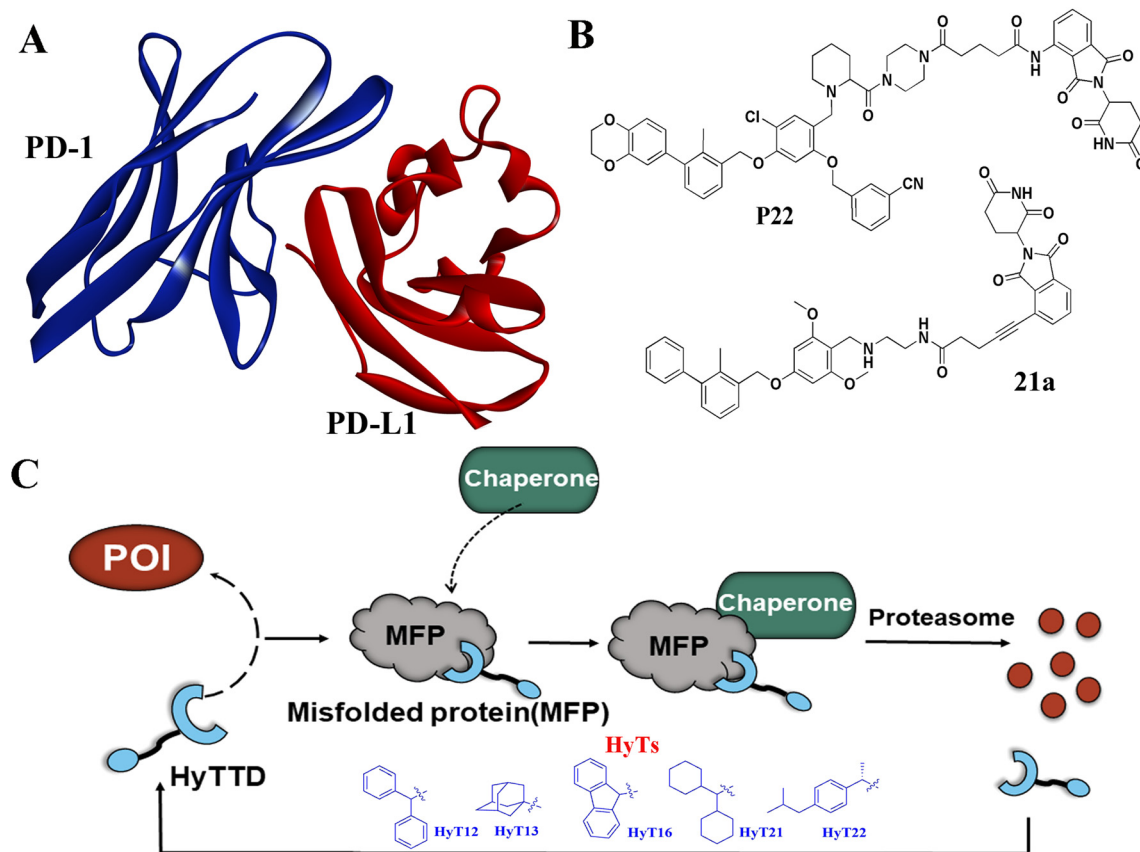
‡ These authors contributed equally.

Fig. 1 The strategies to develop PD-L1 degraders. A) The complex of PD-1 and PD-L1 (PDB-ID:4ZQK); B) the PD-L1 degraders linked with the cereblon ligand; C) the proposed mechanism for HyTTD to degrade the targeted protein.

Design and chemical synthesis of PD-L1 HyTTDs

Various PD-L1 binders have been reported. Among the binders, the biphenyl derivatives exhibit high affinities to PD-L1 by inducing the formation of PD-L1 dimers, thereby blocking the interaction between PD-L1 and PD-1. Therefore, similar to **P22** or **21a** (Fig. 1B), we selected the biphenyl derivatives **BMS-220** and **R3** as the PD-L1 binding motif for PD-L1 considering the high binding affinities with PD-L1 and ease of synthesis (structures shown in Tables 1 and 3).[15,25] It has been identified that the biphenyl group of these compounds is buried in the interface site of the PD-L1 dimer,[26] and the other terminal of the compounds extends to the outside of the site, which is suitable for inducing the linker and HyTs to mimic the unnatural state of PD-L1.

Firstly, we synthesized the PD-L1 binding motifs derived from **BMS-220** and **R3** according to Schemes S1 and S2 (ESI† data), and the corresponding aldehydes (compound **7** and compound **11**) were prepared for further attaching. The linkers (NL_n) were synthesized according to Scheme S3 (ESI† data) through Gabriel's reaction. While linkers CL_n were obtained by cyclic dianhydrides reacting with mono-Boc-protection diamines (Scheme S3†). The PD-L1 binding motifs were attached to the linker through indirect reductive amination, and the HyT motifs were joined to the other end
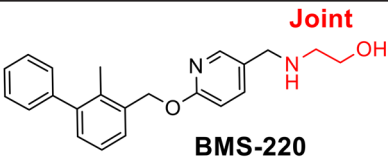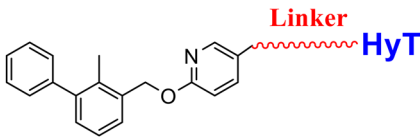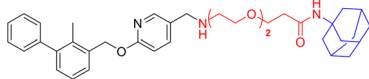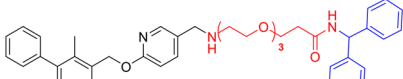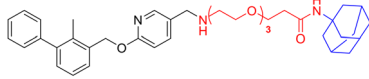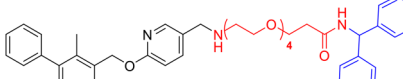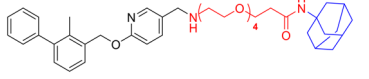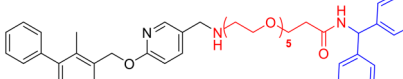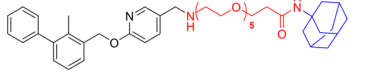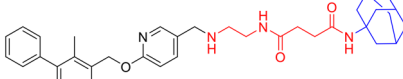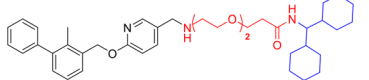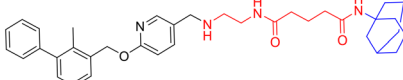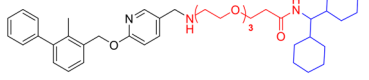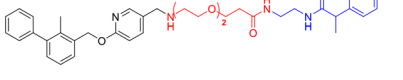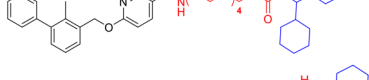
of the linkers through the amide condensation reaction to get the final HyTDDs (Scheme S4, ESI† data).

The introducing of the diphenylmethyl HyT leads to the decrease of PD-L1 protein level

Firstly, we try to develop the PROTACs from the PD-L1 ligand **BMS-220** linked with the von Hippel–Lindau (VHL) ligand, such as **L1V–L5V** (Table S1†). However, such molecules exhibited no degradation activity (Fig. S1†). As the hydrophobic tag (HyT) strategy is more robust and less dependent on the unique E3 ligase than PROTAC technology, we then tried to develop HyTTD which targets the PD-L1 protein. According to the reported HyTs, such as HyT12, HyT13, HyT16, HyT21, and HyT22,[24] we designed the HyTTD compounds in Table 1. We chose the PD-L1 binder **BMS-220** as the motif to bind with PD-L1, and poly (ethylene glycol) (PEG) as the linker to attach the different HyTs (Table 1) to generate compounds **L2a–L5a**, **L2b–L5b**, **L2c–L5c**, and **L2h–L5h**. Furthermore, we designed two 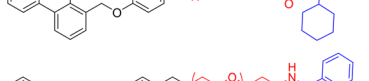other HyTTDs, **LC1a** and **LC2a**, of which the linkers are alkyl chains. From the structures in Table 1, we would like to identify the suitable HyT that induces the degradation activity.

To determine the degradation efficacy of compounds in Table 1, we further checked PD-L1 protein levels in NCI-H460 cells under 10 μM compounds treated through western blot.

Table 1 The HyTTDs from **BMS-220** linked with HyTs HyT12, HyT13, HyT16, HyT21, or HyT22

Compounds	Structure	Compounds	Structure
L2a		L3c	
L3a		L4c	
L4a		L5c	
L5a		LC1a	
L2b		LC2a	
L3b		L2h	
L4b		L3h	
L5b		L4h	
L2c		L5h	

CDK5 inhibitor would lead to the reduction of PD-L1.[27] Therefore, we selected CDK5 inhibitor dinaciclib as the positive control. As demonstrated in Fig. 2A, compounds **L2c**, **L3c**, **L4c**, and **L5a** reduced PD-L1 protein levels after the treatment for 24 h, compared to DMSO treated group. Further dose-dependent assay indicated that **L2c** and **L3c** showed mild degradation potency of PD-L1. From the results, we found that the inducing of HyTs HyT13, HyT16, HyT21, and HyT22 to the designed compounds would not lead to the reducing of PD-L1 protein level. The introducing of HyT12, the diphenylmethyl group, to compounds **L2c** and **L3c** exhibited a decrease in the PD-L1 protein levels. The results indicated that different HyTs may show diverse effects on the degradation of the protein, which was consistent with our previous summary that HyTTDs with different HyTs would lead to distinct degradation effects.[17] Moreover, such results provided a clue in the optimization of the HyTTDs of PD-L1s by the modification of the diphenylmethyl HyTs.

The substituted diphenylmethyl HyT make better degradation activity for PD-L1 HyTTDs

The fluorine substitution is often used in drug development to improve the potency and metabolic stability of lead compounds. Considering that the introducing of HyT12 (diphenylmethyl group) to the HyTTDs will lead to the decrease of PD-L1 level, we next designed and synthesized the HyTTDs with the fluorine or trifluoromethyl substituted diphenylmethyl HyTs such as **L2d–L4d**, **L2e–L4e**, and **L2f–L4f** (Table 2). Moreover, it was reported that the binding affinity to the POI would play a key role in the degradation potency of HyTTDs.[17,28] Therefore, we designed and synthesized the
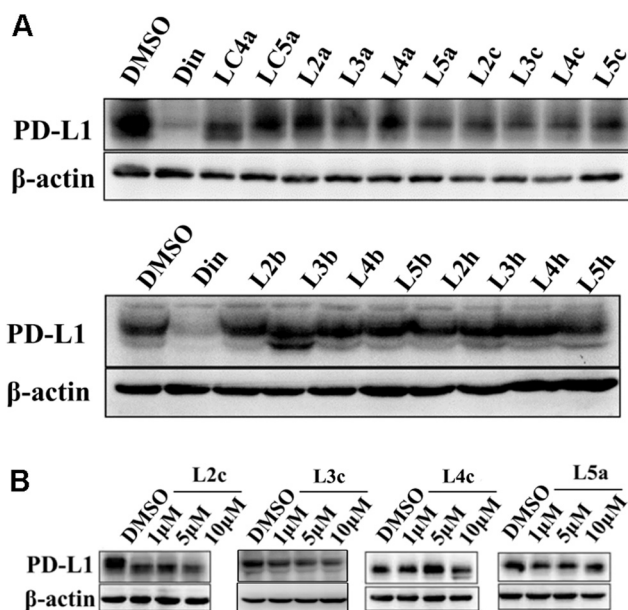
Fig. 2 The effects of designed HyTTDs on the PD-L1 protein level. A) The protein level of PD-L1 treated by various HyTTDs; B) the effects of **L2c**, **L3c**, **L4c**, or **L5a** on the PD-L1 protein level with different concentrations.
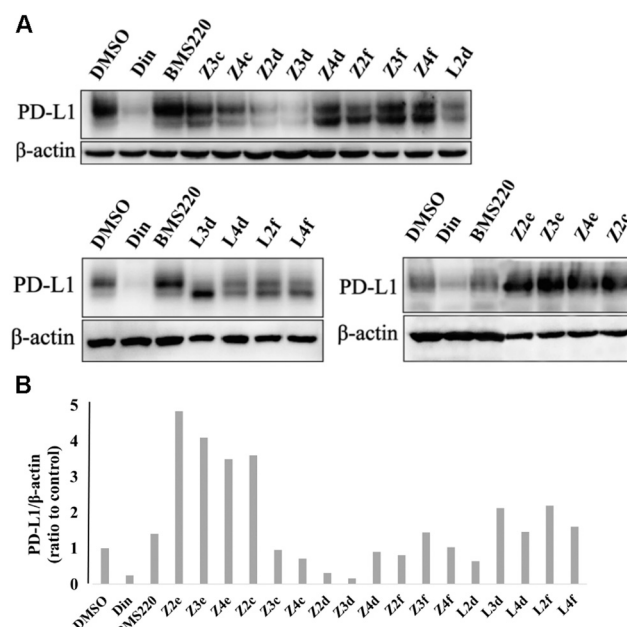

Fig. 3 The effects of designed HyTTDs with substituted diphenylmethyl HyT on the PD-L1 protein level. A) The protein level of PD-L1 treated by various HyTTDs; B) The protein levels were semi-quantified through the ImageJ software.

HyTTDs with the binding motif to PD-L1 replaced **BMS-220** by **R3**, which includes **Z2c–Z4c**, **Z2d–Z3d**, **Z2e–Z4e**, and **Z2f–Z4f** (Table 3).

Next, we detected PD-L1 protein levels in NCI-H460 cells treated with 10 μM compounds listed in Tables 2 and 3 through western blot. As a result, compared to the DMSO or **BMS-220** treated group, compound **Z3c**, **Z4c**, **Z2d**, **Z3d**, or **L2d** treated group showed a decrease in PD-L1 protein level (Fig. 3A). The **Z2d**, **Z3d**, or **L2d** treated group exhibited a comparable potency to that of dinaciclib as the result of the quantification by ImageJ (Fig. 3B). These three compounds **Z2d**, **Z3d**, and **L2d** all bear 4,4′-bifluorobenzhydrylpiperazinyl HyT, which belong to a novel HyT. Interestingly, through the query from the Drugbank (https://go.drugbank.com),[29] we found that two approved drugs flunarizine and almitrine bearing 4,4′-bifluorobenzhydrylpiperazinyl motifs, which indicated that such a HyT group could be applied in the drug development.

The confirmation assay for HyTTDs activities

Further western blot assay indicated that compounds **Z2d**, **Z3d**, and **L2d** could reduce the protein levels of PD-L1 in a dose-dependent mode (Fig. 4A), which confirmed previous results. Moreover, **Z2d** showed a significant decrease in PD-L1 level at the concentration of 1 μM. To verify if the decrease in PD-L1 was caused by the cytotoxicity, the MTT assay was performed for the NCI-H460 cells treated by **Z2d**, **Z3d**, or **L2d**. As a result, the compound **L2d** showed mild cytotoxicity at 10 μM, while **Z2d** and **Z3d** indicated almost no cytotoxicity at the concentration range from 0.5 μM to 10 μM (Fig. 4B), which
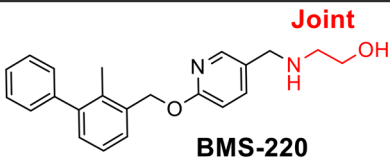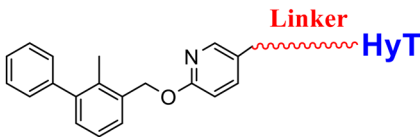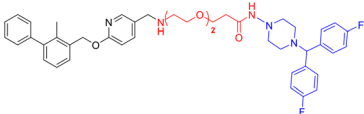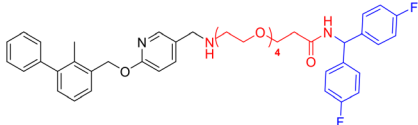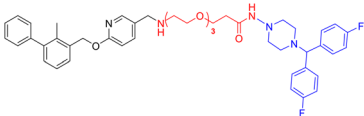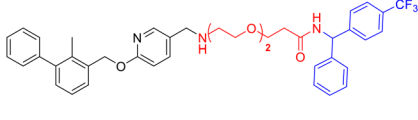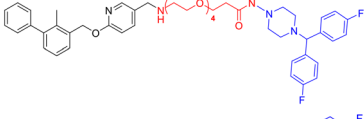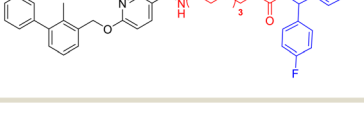
indicated that the decrease in the PD-L1 level was not caused by the toxicity of **Z2d** or **Z3d**. In our previous work, we identified a cell line HT-1080 expressing a significantly higher level of PD-L1 than other cell lines including NCI-H460.[30] Therefore, we tested if **Z2d** and **Z3d** would downregulate the PD-L1 protein level in HT-1080. As a result, **Z2d** or **Z3d** treated groups showed a decrease in PD-L1 level in a dose-dependent mode (from 1 to 10 μM, Fig. S2†), which indicated that **Z2d** or **Z3d** could reduce the protein level of PD-L1 in diverse cell lines.

Next, the immunofluorescence assay was further performed to evaluate the effects of the compounds **Z2d** and **Z3d** on the level of PD-L1. NCI-H460 cells were treated with **Z2d** or **Z3d** in different concentrations. The cells were incubated with primary antibody to PD-L1 and followed by Alexa Fluor-conjugated secondary antibody, and nuclei were visualized by DAPI staining. As results, the immunofluorescence staining experiments showed that both **Z2d** and **Z3d** could inhibit the PD-L1 protein levels of NCI-H460 cells in a dose-dependent manner (Fig. 5). **Z2d** and **Z3d** could down-regulate the protein levels of PD-L1 at the concentration of 10 μM, which was comparable to the pos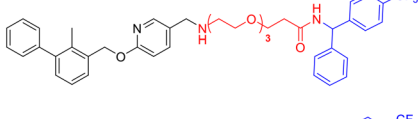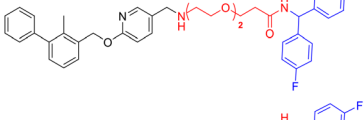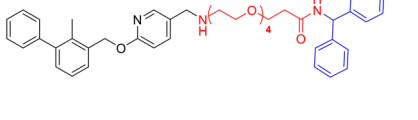itive control dinaciclib. Therefore, both western blot and immunofluorescence assay indicated that **Z2d** and **Z3d** could down-regulate the PD-L1 protein levels.

Z2d/Z3d promoted PD-L1 degradation through proteasome pathway

The proteasome pathway is the main participant that regulates intracellular protein degradation. It was reported that HyTTD-induced protein degradation was dependent on

Table 2 The HyTTDs from **BMS-220** were linked with substituted diphenylmethyl HyT

Compounds	Structure	Compounds	Structure
L2d		**L4e**	
L3d		**L2f**	
L4d		**L3f**	
L2e		**L4f**	
L3e			

the proteasome pathway.[28] To explore whether **Z2d**/**Z3d** promoted PD-L1 degradation through the proteasome pathway, NCI-H460 cells were treated with **Z2d**/**Z3d** in the presence or absence of proteasome inhibitor **MG132**. As a result (Fig. 6A), the reduction of PD-L1 protein levels by **Z2d**/**Z3d** was counteracted by **MG132**, which indicated that **Z2d**/**Z3d** degraded PD-L1 through the proteasome pathway. Meanwhile, the time-course effects of **Z2d**/**Z3d** for PD-L1 down-regulation were evaluated at the concentration of 10 μM. Unfortunately, either **Z2d** or **Z3d** exhibited reduced degradation activity for PD-L1 in NCI-H460 cells over time, and there was almost no degradation activity for 72 h, which indicated that the **Z2d** or **Z3d** might be unstable in cell culture conditions.
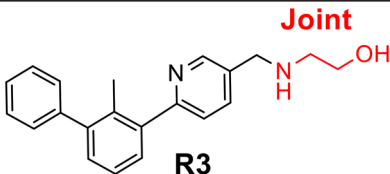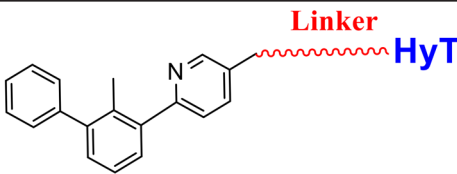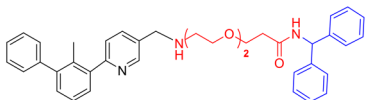
The predicted binding mode between Z2d or Z3d with PD-L1

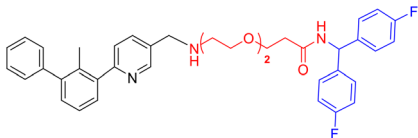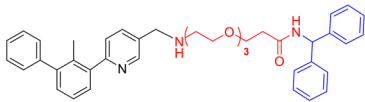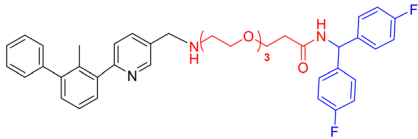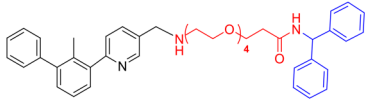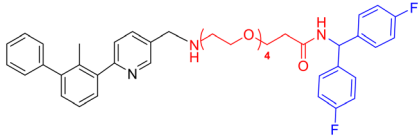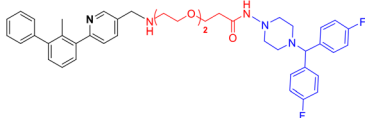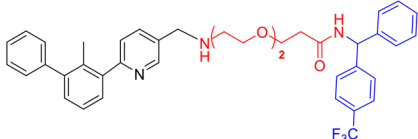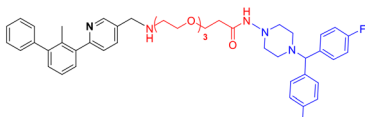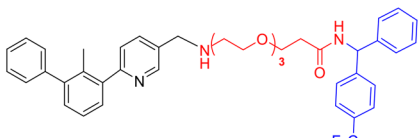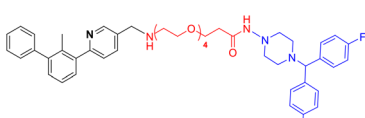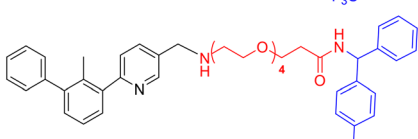We further investigated the binding mode of **Z2d** or **Z3d** with PD-L1, and the binding modes of **Z2d** or **Z3d** in the PD-L1 site were predicted through molecular docking using the DOCK module in MOE. Using the crystal structure of the PD-L1 and compound **HOU** (PDB code: 7DY7)[31] as the receptor structure for docking, both **Z2d** and **Z3d** were docked into the binding site occupied by compound **HOU**, and the results were shown in Fig. 7. The two compounds adopted similar orientations in the binding site composed by PD-L1 dimer with the biphenyl group at the subsite formed by hydrophobic residues

including Ile 54 (A chain), Ala 121 (B chain), Met 115 (A and B chains), and Ile 116 (A and B chains), also similar to that of compound **HOU**. The PEG linkers of both compounds were extended to the upper part of the binding site and formed a hydrogen bond with Lys 124 (B chain). Particularly, the HyTs were stretched into the solvent for both compounds, which was supposed to mimic unnatural state proteins to induce the degradation (Fig. 7). Our molecular modeling results indicated that the attachment of two or three glycol-linked chains and 4,4′-bifluorobenzhydrylpiperazinyl HyT would not affect the binding mode of the PD-L1 binding motif (compared to the compound **HOU**), and such a long linker (two or three glycol linked chains) also allowed the HyT group extending the surface of the protein to mimic the misfold.

Discussion

Herein we designed and synthesized a series of PD-L1 HyTTDs with different linkers, different HyTs, and the different PD-L1 binder motifs derived from **BMS-220** and **R3**. Among the compounds, **Z2d** and **Z3d** showed good degradation activity for PD-L1 in multiple cell lines including NCI-H460 and H-1080. Moreover, our work indicated that the linker type or HyT type has a great effect on the degradation activity of the PD-L1 HyTTDs. We found that the inducing of the diphenylmethyl HyTs had the degradation potency for PD-L1, and further modification of the diphenylmethyl HyTs

Table 3 The HyTTDs from **R3** linked with substituted diphenylmethyl HyT

Compounds	Structure	Compounds	Structure
Z2c		Z2e	
Z3c		Z3e	
Z4c		Z4e	
Z2d		Z2f	
Z3d		Z3f	
Z4d		Z4f	

led to the HyTTD with the better degradation potency. Importantly, we developed several HyTs through the modification of the diphenylmethyl group and identified the 4,4′-bifluorobenzhydrylpiperazinyl group as the novel HyT for the development of PD-L1 HyTTD. Such a HyT could be applied to develop the HyTTD for other target proteins.

TPD strategy has been applied to develop the inhibitor of PD-1 and PD-L1 interaction, such as recently reported compounds **21a**, **P22**, and **F4**.[20,21,32] The HyTTD technology is a valuable complement to PROTAC technology with more robust and less dependent on the unique E3 ligase than PROTAC technology. According to the current degrading mechanism, the HyTTD could degrade the intracellular PD-L1 rather than the cell-surface PD-L1. Interestingly, the degradation of intracellular PD-L1 also led to a decrease of cell surface PD-L1.[20] The intracellular PD-L1 is a reservoir for the replenishment of antibody-degraded membrane PD-L1, the degradation of intracellular PD-L1 could lead to more effective cancer immunotherapy. Meanwhile, it is reported that the cytoplasmic domain of PD-L1 can regulate PD-L1 stability and function through multiple pathways. Therefore, the intracellular domain of PD-L1 and its regulatory pathways could be promising targets for cancer therapy, expanding available strategies for combined immunotherapy.[33] Moreover, the intracellular PD-L1 increases mRNA expression of factors regulating the DNA damage response (DDR), which in turn contributes to tumor cell resistance to radiotherapy and chemotherapy.[34] Combined targeting of the intracellular and extracellular functions of PD-L1 may represent a promising approach that enhances the antitumor immune activity.

However, the degradation potency of HyTTDs is not significant compared to PROTAC.[17,28] In the case of PD-L1 as POI, our developed HyTTDs exhibited promising activity in degrading the protein of PD-L1, which indicated that HyTTD technology was a potential strategy to develop the PD-L1 degraders, and the further optimization and *in vivo*
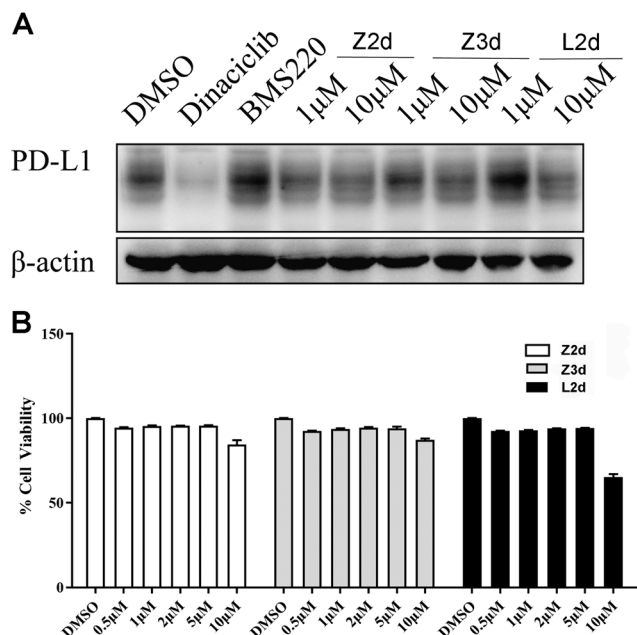
A

B

Fig. 4 The confirmation assay for HyTTDs activities. A) The effects of **Z2d**, **Z3d**, or **L2d** on the PD-L1 protein level with different concentrations; B) the cytotoxicity of **Z2d**, **Z3d**, or **L2d** by the MTT assay for the NCI-H460 cells.

evaluation should be performed to obtain the HyTTD PD-L1 degraders with better potency.[17] It was reported that PROTAC **21a** downregulated PD-L1 protein in a proteasome-dependent manner.[21] Surprisingly, although designed as the PROTAC, **P22** reduces the protein levels of PD-L1 in a lysosome-dependent manner.[20] As for our HyTTDs, current data support that both **Z2d** and **Z3d** downregulate PD-L1 levels in a proteasome-dependent manner, however, the precise mechanisms of HyTTD-induced PD-L1 degradation remain unclear.

Methods

General procedure for the synthesis of HyTTDs

The synthetic routes for PD-L1 binder motifs and linkers were referred to Schemes S1–S3 (ESI† data). The detailed synthesis procedures of the HyTTDs (Scheme S4†) and the detailed spectral data were listed in the ESI.† Herein, we listed the procedure of the synthesis of **L2a**–**L5i** as examples.

Compound **7** (PD-L1 binder motif derived from **BMS-220**) was dissolved in methanol under a nitrogen atmosphere, then the linkers **NL2**–**NL5** were added dropwise to the solution and stirred overnight at 40 °C. NaBH$_4$ (3.0 eq.) was added and the solvent was evaporated under reduced pressure, and the crude product was separated by column chromatography to give compound **17**.

Compound **17** (compound **18**) was dissolved in DCM, then TFA was added dropwise to form TFA : DCM (1 : 1), stirred at room temperature for 2 h. The solvent was evaporated under

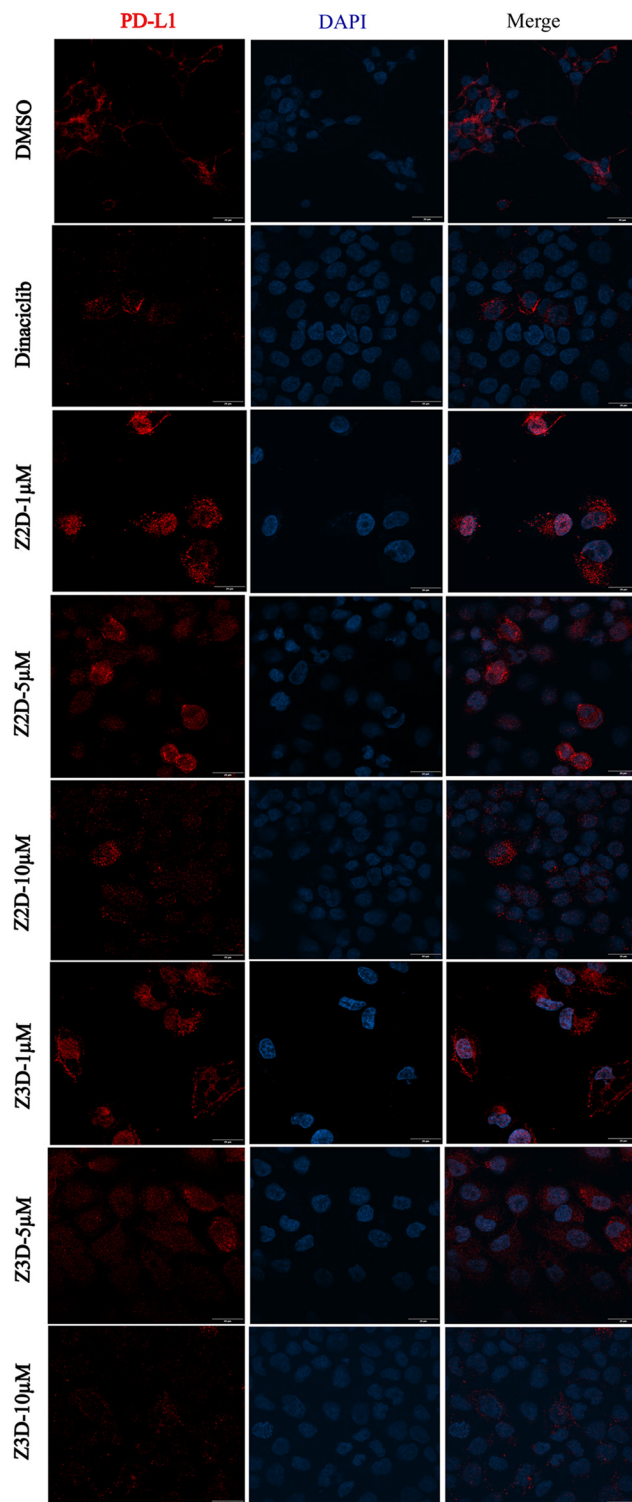**Fig. 5** Immunofluorescence staining of PD-L1 (red) in NCI-H460 cells treated with **Z2d** and **Z3d** in different concentrations. Nuclei were visualized by DAPI staining (blue).

reduced pressure to obtain the crude product compound **19**, and the crude product was used directly in the next step.

Compound **19**, HATU (1.5 eq.), and DIPEA (5.0 eq.) were dissolved in DCM, and R^3–NH$_2$ (R^3 = a–i, 1.0 eq.) dissolved in
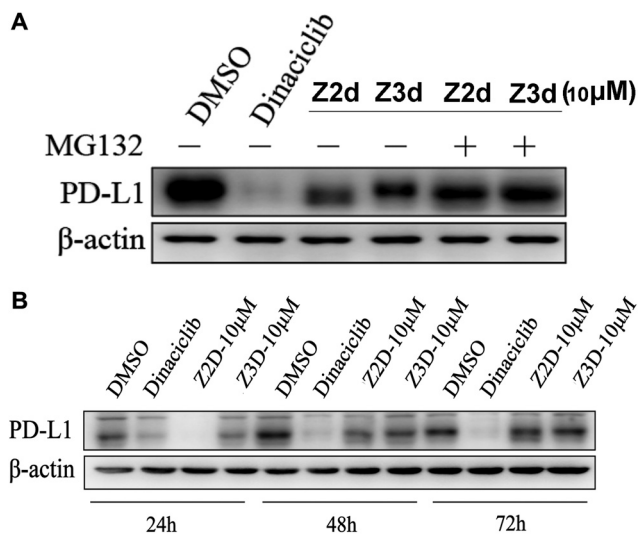
A

B

Fig. 6 A) Western blot analysis of PD-L1 protein levels 10 μM **Z2d/Z3d** or/and 5 μM MG132; B) the time-course effects of **Z2d/Z3d** for PD-L1 down-regulation.

DCM was added dropwise and stirred at room temperature for 3 hours. The organic phase extract was dried over anhydrous sodium sulfate, the solvent was evaporated under reduced pressure, and the crude product was separated by column chromatography to give hydrophobic labeled compounds **L2a–L5i.**

Cell culture

NCI-H460 and HT-1080 cell lines were purchased from American Type Culture Collection (ATCC). HT-1080 cells were cultured in minimum essential medium (MEM; Thermo Fisher Scientific) with 10% fetal bovine serum (FBS; Gibco) at 37 °C in a 5% CO_2 incubator, and H-460 cells were cultured in Roswell Park Memorial Institute – 1640 (RPMI-1640; Thermo Fisher Scientific) with 10% fetal bovine serum (FBS; Gibco) at 37 °C in a 5% CO_2 incubator.

Western blot

HT-1080 cells were seeded at a density of 1×10^6 cells per well in a 6-well plate. After overnight incubation, 2 μL DMSO (Sigma-Aldrich) or 2 μL chemical compounds with different concentrations were added to each well at the designated concentration. After another 24 h incubation, the cells were lysed with RIPA. Then the protein lysis was denatured at 100 °C in SDS-PAGE loading buffer for 15 min was treated and separated by 10% SDS-PAGE. The membranes were probed with primary antibodies against PD-L1 overnight at 4 °C. All antibodies were purchased from Cell Signaling Technology and diluted at a ratio of 1 : 1000. Mouse anti-β-actin (1 : 5000, Abcam) was used as a loading control. Proteins were visualized using anti-mouse or anti-rabbit HRP-conjugated
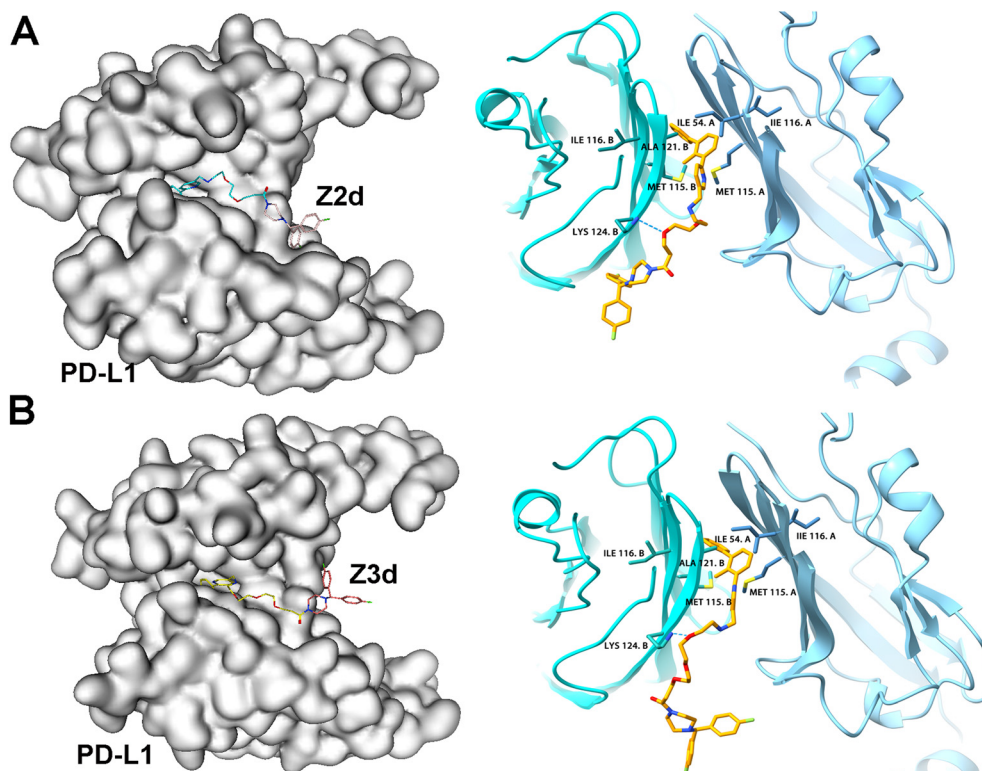
Fig. 7 The predicted binding mode between **Z2d** or **Z3d** with PD-L1. A) The binding mode and detailed interactions between the **Z2d** and PD-L1. The PD-L1 is in surface and the **Z2d** is in stick; B) the binding mode and detailed interactions between the **Z3d** and PD-L1. The PD-L1 is in the surface and the **Z3d** is in stick. The ligand–protein interaction illustrations were performed with UCSF ChimeraX. The hydrogen bond is indicated by a blue dash.

secondary antibodies (1 : 5000, Zhongshan Jinqiao Biotechnology Company) and ECL-Plus (Millipore).

Immunofluorescence

Cells were fixed in 4% paraformaldehyde (in 1× PBS) for 15 min at room temperature, and then washed with 1× PBS three times. After blocking with 0.5% BSA for 1 h, the cells were incubated with primary antibody to PD-L1 (ab205921, 1 : 200, Abcam, USA) overnight at 4 °C with gentle shaking. After washing with 1× PBS three times, Alexa Fluor-conjugated secondary antibodies (Alexa Fluor 555 – donkey anti-rabbit) (1 : 1000, Life Technologies, Shanghai China) were added for a further incubation of 30 min in dark. Nucleus were stained with DAPI (4′,6-diamidino-2-phenylindole). Images were recorded with a PerkinElmer Ultra View VoX confocal imaging system.

MTT assay

NCI-H460 cells were seeded at a density of 4×10^3 cells per well in 96-well plates in the complete RPMI-1640 growth medium, after 24 h incubation, 1 μL DMSO (Sigma-Aldrich) or 1 μL chemical compounds at different concentration were added to each well. After 24 h, 48 h, and 72 h incubation, 20 μL MTT solution (5 mg mL^{-1} in PBS) was added to each well and incubated for another 4 h. The MTT formazan formed by metabolically viable cells was dissolved in 100 μL isopropanol. The absorbance was measured at 570 nm wavelength on a plate reader (EnSpire 2300, PerkinElmer). Experiments were performed in triplicate. The value of the DMSO group was defined as 100%.

Molecular modeling

The binding mode for **Z2d** or **Z3d** in the binding site of PD-L1 (PDB code: 7DY7) was generated through molecular docking using MOE (Molecular Operating Environment) version 2009.10. In general, the docking was performed through the 'DOCK' module in MOE using the alpha-triangle placement method. 2000 poses were generated during molecular docking. Refinement of the docked poses was carried out using the force field refinement scheme and scored using both the affinity dG and London dG scoring system. The pose with the highest docking score was returned for further analysis. The ligand–protein interaction illustrations were performed with UCSF ChimeraX.[35]

Statistical analysis

Data are presented as mean standard deviation (SD) from at least three independent experiments. Statistical analyses were performed using a two-tailed Student's *t*-test, or one-way ANOVA with Dunnet's *post hoc* test for multiple comparisons by using SPSS software (version 25.0.IBM Corp., Armonk, NY, USA) as appropriate. *P* values ≦ of 0.05 were considered significant. * denotes $p \leqq 0.05$, ** indicates $p \leqq 0.01$.

Data availability

The data supporting this article have been included as part of the ESI.†

Author contributions

The manuscript was written through the contributions of all authors. All authors have approved the final version of the manuscript.

Conflicts of interest

There is no conflict of interest to declare.

References

1 R. H. Thompson, H. Dong, C. M. Lohse, B. C. Leibovich, M. L. Blute, J. C. Cheville and E. D. Kwon, *Clin. Cancer Res.*, 2007, **13**, 1757–1761.

2 Y. Zhang, S. Huang, D. Gong, Y. Qin and Q. Shen, *Cell. Mol. Immunol.*, 2010, **7**, 389–395.

3 N. Boisgerault and P. Bertrand, *Eur. J. Med. Chem.*, 2023, **256**, 115465.

4 P. Sharma, S. Goswami, D. Raychaudhuri, B. A. Siddiqui, P. Singh, A. Nagarajan, J. Liu, S. K. Subudhi, C. Poon, K. L. Gant, S. M. Herbrich, S. Anandhan, S. Islam, M. Amit, G. Anandappa and J. P. Allison, *Cell*, 2023, **186**, 1652–1669.

5 C. Sun, R. Mezzadra and T. N. Schumacher, *Immunity*, 2018, **48**, 434–452.

6 F. K. Dermani, P. Samadi, G. Rahmani, A. K. Kohlan and R. Najafi, *J. Cell. Physiol.*, 2019, **234**, 1313–1325.

7 G. I. Vladimer, B. Snijder, N. Krall, J. W. Bigenzahn, K. V. M. Huber, C. H. Lardeau, K. Sanjiv, A. Ringler, U. W. Berglund, M. Sabler, O. L. de la Fuente, P. Knöbl, S. Kubicek, T. Helleday, U. Jäger and G. Superti-Furga, *Nat. Chem. Biol.*, 2017, **13**, 681–690.

8 A. Ribas and J. D. Wolchok, *Science*, 2018, **359**, 1350–1355.

9 H. F. Zhu and Y. Li, *Nat. Prod. Bioprospect.*, 2018, **8**, 297–301.

10 B. Cheng, Y. Xiao, M. Xue, H. Cao and J. Chen, *J. Med. Chem.*, 2020, **63**, 15389–15398.

11 P. Zhu, J. Zhang, Y. Yang, L. Wang, J. Zhou and H. Zhang, *Mol. Diversity*, 2022, **26**, 245–264.

12 J. Guo, L. Luo, Z. Wang, N. Hu, W. Wang, F. Xie, E. Liang, X. Yan, J. Xiao and S. Li, *J. Med. Chem.*, 2020, **63**, 13825–13850.

13 S. Basu, J. Yang, B. Xu, K. Magiera-Mularz, L. Skalniak, B. Musielak, V. Kholodovych, T. A. Holak and L. Hu, *J. Med. Chem.*, 2019, **62**, 7250–7263.

14 K. Guzik, K. M. Zak, P. Grudnik, K. Magiera, B. Musielak, R. Torner, L. Skalniak, A. Domling, G. Dubin and T. A. Holak, *J. Med. Chem.*, 2017, **60**, 5857–5867.

15 T. Wang, S. Cai, M. Wang, W. Zhang, K. Zhang, D. Chen, Z. Li and S. Jiang, *J. Med. Chem.*, 2021, **64**, 7390–7403.

16 R. R. Paudel, D. Lu, S. Roy Chowdhury, E. Y. Monroy and J. Wang, *Biochemistry*, 2023, **62**, 564–579.

17 J. Gao, J. Zhang, X. Han and J. Zhou, *Curr. Med. Chem.*, 2023, **30**, 3137–3155.

18 L. Zhao, J. Zhao, K. Zhong, A. Tong and D. Jia, *Signal Transduction Targeted Ther.*, 2022, **7**, 113.

19 P. P. Chamberlain and L. G. Hamann, *Nat. Chem. Biol.*, 2019, **15**, 937–944.

20 B. Cheng, Y. Ren, H. Cao and J. Chen, *Eur. J. Med. Chem.*, 2020, **199**, 112377.

21 Y. Wang, Y. Zhou, S. Cao, Y. Sun, Z. Dong, C. Li, H. Wang, Y. Yao, H. Yu, X. Song, M. Li, J. Wang, M. Wei, G. Yang and C. Yang, *Bioorg. Chem.*, 2021, **111**, 104833.

22 S. Xie, F. Zhan, J. Zhu, Y. Sun, H. Zhu, J. Liu, J. Chen, Z. Zhu, D. H. Yang, Z. S. Chen, H. Yao, J. Xu and S. Xu, *Angew. Chem., Int. Ed. Engl.*, 2023, **62**, e202217246.

23 S. Xie, J. Zhu, J. Li, F. Zhan, H. Yao, J. Xu and S. Xu, *J. Med. Chem.*, 2023, **66**, 10917–10933.

24 T. K. Neklesa, H. S. Tae, A. R. Schneekloth, M. J. Stulberg, T. W. Corson, T. B. Sundberg, K. Raina, S. A. Holley and C. M. Crews, *Nat. Chem. Biol.*, 2011, **7**, 538–543.

25 Bristol-Myers Squibb Company, *USA Pat.*, WO2015034820A1, 2015.

26 K. Guzik, K. M. Zak, P. Grudnik, K. Magiera, B. Musielak, R. Törner, L. Skalniak, A. Dömling, G. Dubin and T. A. Holak, *J. Med. Chem.*, 2017, **60**, 5857–5867.

27 R. D. Dorand, J. Nthale, J. T. Myers, D. S. Barkauskas, S. Avril, S. M. Chirieleison, T. K. Pareek, D. W. Abbott, D. S. Stearns, J. J. Letterio, A. Y. Huang and A. Petrosiute, *Science*, 2016, **353**, 399–403.

28 Q. He, X. Zhao, D. Wu, S. Jia, C. Liu, Z. Cheng, F. Huang, Y. Chen, T. Lu and S. Lu, *Eur. J. Med. Chem.*, 2023, **260**, 115741.

29 D. S. Wishart, Y. D. Feunang, A. C. Guo, E. J. Lo, A. Marcu, J. R. Grant, T. Sajed, D. Johnson, C. Li, Z. Sayeeda, N. Assempour, I. Iynkkaran, Y. Liu, A. Maciejewski, N. Gale, A. Wilson, L. Chin, R. Cummings, D. Le, A. Pon, C. Knox and M. Wilson, *Nucleic Acids Res.*, 2018, **46**, D1074–D1082.

30 Y. Xie, J. Ding, X. Cui, M. Wu, C. Huang, R. Zhang, J. Wang, X. Li, S. Cen and J. Zhou, *Eur. J. Pharm. Sci.*, 2020, **142**, 105088.

31 T. Wang, S. Cai, Y. Cheng, W. Zhang, M. Wang, H. Sun, B. Guo, Z. Li, Y. Xiao and S. Jiang, *J. Med. Chem.*, 2022, **65**, 3879–3893.

32 C. Pan, M. Luo, Y. Lu, X. Pan, X. Chen, L. Ding, J. Che, Q. He and X. Dong, *Bioorg. Chem.*, 2022, **125**, 105820.

33 F. Chai, P. Li, X. Liu, Z. Zhou and H. Ren, *J. Mol. Cell Biol.*, 2023, **15**(11), mjad070.

34 X. Tu, X. Qin, B. Zhang, Y. Zhang, C. Zhang, M. Kahila, S. Nowsheen, P. Yin, J. Yuan, H. Pei, H. Li, J. Yu, Z. Song, Q. Zhou, F. Zhao, J. Liu, C. Zhang, H. Dong, R. W. Mutter and Z. Lou, *Mol. Cell*, 2019, **74**, 1215–1226.e1214.

35 E. C. Meng, T. D. Goddard, E. F. Pettersen, G. S. Couch, Z. J. Pearson, J. H. Morris and T. E. Ferrin, *Protein Sci.*, 2023, **32**, e4792.